Interdecadal Variability of ENSO in 21 IPCC AR4 Coupled GCMs

Jia-Lin Lin

NOAA ESRL/CIRES Climate Diagnostics Center, Boulder, CO

Geophys. Res. Lett.
Revised, February 2007

Corresponding author address: Dr. Jia-Lin Lin
NOAA ESRL/CIRES Climate Diagnostics Center
325 Broadway, R/PSD1, Boulder, CO 80305-3328
Email: jialin.lin@noaa.gov
Web: http://www.cdc.noaa.gov/people/jialin.lin/

Abstract

This study evaluates the interdecadal variability of ENSO in 21 IPCC AR4 CGCMs. 110 years of the Climate of the 20th Century (20C3M) simulations are analyzed using wavelet analysis. The results show that the state-of-the-art CGCMs display a wide range of skill in simulating the interdecadal variability of ENSO. The 21 models can be categorized into three groups. The first group (8 models) shows an oscillation with a constant period shorter than the observed ENSO period, and sometimes with a constant amplitude. The second group (6 models) does not produce many statistically significant peaks in the ENSO frequency band, but usually produces one or two prominent peaks (episodes) at period longer than 6 years. The third group (8 models) displays significant interdecadal variability of ENSO in both amplitude and period. Moreover, the MPI model even reproduces the observed eastward shift of the westerly anomalies in the low-frequency regime.

1. Introduction

Many observational studies have shown that the El Nino/Southern Oscillation (ENSO) displays significant interdecadal variability in its amplitude, period and onset (e.g. Gu and Philander 1995; Wang 1995; Mak 1995; Wang and Wang 1996; Torrence and Compo 1997). Several theories have been developed to explain ENSO's interdecadal variability, such as oceanic teleconnections (e.g. Gu and Philander 1997; Kleeman et al. 1999), atmospheric teleconnections (e.g. Barnett et al. 1999) and structure of the coupled mode (e.g. An and Wang 2000). From observational data, An and Wang (2000) found that the frequency change of ENSO is accompanied by a significant change in ENSO structure with an eastward shift of the westerly anomalies in the low-frequency regime. They further use a theoretical model to demonstrate the underlying physical mechanism based on the relative contribution of the thermocline feedback and zonal advection feedback.

Many studies have evaluated the ENSO simulations of coupled general circulation models (CGCMs; e.g. Delecluse et al. 1998; Latif et al. 2001; Davey et al. 2002; AchutaRao and Sperber 2002, 2006). However, the ability of CGCMs to simulate ENSO's interdecadal variability has not been evaluated. This is important because if there are some CGCMs that can produce interdecadal variability of ENSO, they may help us to understand the physical mechanisms of this variability.

Recently, in preparation for the Inter-governmental Panel on Climate Change (IPCC) Fourth Assessment Report (AR4), more than 20 state-of-the-art CGCMs produce a comprehensive set of long-term simulations for both the 20th century's climate and different climate change scenarios in the 21st century. The purpose of this study is to

evaluate the simulations of ENSO's interdecadal variability in 21 IPCC AR4 CGCMs. The models and validation datasets used in this study are described in section 2. The diagnostic methods are described in section 3. Results are presented in section 4. A summary and discussion are given in section 5.

2. Data and method

This analysis is based on 110 years of the Climate of the 20th Century (20C3M) simulations from 21 CGCMs (e.g. Boyle 2006; Lin 2006; Lin et al. 2006). See Lin (2006; his Table 1) for the model names and acronyms, their horizontal and vertical resolutions, and brief descriptions of their deep convection schemes. For each model we use 110 years of monthly mean surface skin temperature (SST).

To sample the uncertainties associated with SST measurements/retrievals, we use two different observational datasets to validate the model simulations: (1) the Extended Reconstruction of SST (ERSST; Smith and Reynolds 2004), and (2) the Met Office Hadley Centre's Sea Ice and SST (HADISST; Rayner et al. 2003). Both datasets are monthly data covering 110 years (1890-1999), and with a horizontal resolution of 1 degree longitude by 1 degree latitude.

Following the previous observational studies (e.g. Gu and Philander 1995; Wang 1995; Mak 1995; Wang and Wang 1996; Torrence and Compo 1997), the interdecadal variability of ENSO is analyzed using wavelet analysis. Wavelet analysis is a powerful tool for analyzing multi-scale, nonstationary processes. Its uniqueness is its ability of simultaneously localizing the variability of the signal in both frequency and time domains by using generalized local base functions (wavelets) that can be stretched and translated with a flexible resolution in both frequency and time (e.g. Mak 1995; Torrence and Compo 1997). In other words, one can determine both the dominant modes of variability and how those modes vary in time. We use the wavelet analysis program developed by Torrence and Compo (1997) and use the Morlet wavelet as the mother wavelet.

3. Results

Before conducting the wavelet analysis, we first look at the normalized Fourier spectrum of the Nino3 SST (averaged between 5N-5S, 90W-150W) in both observations and the 21 IPCC AR4 CGCMs (Figure 1). The observed ENSO is a broadband phenomenon with a wide spectral peak between period 3-6 years. The simulations of the 21 CGCMs can be categorized into the following three groups: (1) the first group including 8 models (CCSM3, IAP, HadCM3, MRI, ECHO-G, CNRM, BCCR, and IPSL) which displays a pronounced spectral peak with period shorter than the observed ENSO period; (2) the second group including 5 models (CGCM-T47, CGCM-T63, GISS-AOM, GISS-ER, and MIROC-medres) which have most of their variances distributed at period longer than 6 years; and (3) the third group including 8 models (PCM, GISS-EH, HadGEM1, CSIRO, GFDL2.0, GFDL2.1, MPI, and INM) which produces quite realistic spectral peak of ENSO.

Next we look at the wavelet spectrum of Nino3 SST (Figure 2). Only power above the 95% confidence level is plotted. In observations (Figure 2a, Figure 2b), ENSO displays significant interdecadal variability in its amplitude and period. The amplitude is large before 1915, small between 1915-1950, and large again after 1950. The dominant period is about 3 years before 1910, 4-7 years between 1910-1965, 3-4 years between 1965-1980, and 4-5 years after 1980. These are consistent with the results of previous studies (e.g. Gu and Philander 1995; Wang 1995; Mak 1995; Wang and Wang 1996; Torrence and Compo 1997).

The above three groups of models display different characteristics in their wavelet spectrum. The first group of models generally shows an oscillation with a constant period

shorter than the observed ENSO period, and sometimes with a constant amplitude (e.g. IAP, CNRM). The second group of models does not produce many statistically significant peaks in the ENSO frequency band, but usually produces one or two prominent peaks (episodes) at period longer than 6 years (e.g. GISS-AOM, MIROC-medres). The third group of models generally displays significant interdecadal variability of ENSO in both amplitude and period (e.g. CSIRO, MPI). For example, in the CSIRO model (Figure 2m), the ENSO period varies from 2 years in 1950-1960 to 6 years after 1980. Therefore, we do have a number of CGCMs that can produce interdecadal variability of ENSO. It is important to note that the category boundaries are not necessarily clear-cut. For example, HadCM3 sits somewhere between category 1 and category 3.

As discussed in the introduction, An and Wang (2000) found from observation that the frequency change of ENSO is accompanied by a significant change in ENSO structure with an eastward shift of the westerly anomalies in the low-frequency regime. Does this shift exist in some of the models with interdecadal variability of ENSO? Figure 3 shows the linear correlation with respect to Nino3 SST anomaly for SST anomaly (solid) and zonal wind stress (ZWS) anomaly (dashed) along the equator (5N-5S) for the MPI model. The black lines are for model years 1960-1979 (low-frequency regime; see Figure 2s), the red lines are for model years 1980-1999 (high-frequency regime), and the blue lines are for model years 1940-1959 (another high-frequency regime). Amazingly, Figure 3a looks quite similar to Figure 2 of An and Wang (2000), and the MPI model does reproduce the eastward shift of the westerly anomalies in the low-frequency regime. Therefore, the MPI coupled GCM may be used to study the physical mechanism of this

structure change associated with the interdecadal variability of ENSO to see if it is consistent with the theoretical model of An and Wang (2000), although some cautions need to be taken because the MPI model has the double-ITCZ problem (Lin 2006). No other models in category 3 produce the phase shift (Figure 3b-h). It would be interesting to study why the MPI model behave differently from other models.

4. Summary

This study evaluates the interdecadal variability of ENSO in 21 IPCC AR4 CGCMs. 110 years of the Climate of the 20th Century (20C3M) simulations are analyzed using wavelet analysis. The results show that the state-of-the-art CGCMs display a wide range of skill in simulating the interdecadal variability of ENSO. The 21 models can be categorized into three groups. The first group (8 models) shows an oscillation with a constant period shorter than the observed ENSO period, and sometimes with a constant amplitude. The second group (6 models) does not produce many statistically significant peaks in the ENSO frequency band, but usually produces one or two prominent peaks (episodes) at period longer than 6 years. The third group (8 models) displays significant interdecadal variability of ENSO in both amplitude and period. Therefore, we do have a number of CGCMs that can produce interdecadal variability of ENSO. Among these models, only the MPI model reproduces the observed eastward shift of the westerly anomalies in the low-frequency regime.

These results are very encouraging because detailed analysis of the third group of models, and in-depth intercomparison among the three groups may help us to understand the physical mechanisms of the interdecadal variability of ENSO.

Acknowledgements

We would like to thank Chris Torrence and Gil Compo for the wavelet analysis program. This study was supported by the U.S. CLIVAR CMEP program, NOAA CPO/CVP Program, NOAA CPO/CDEP Program, and NASA Modeling, Analysis and Prediction (MAP) Program.

REFERENCES

AchutaRao, K., and K. R. Sperber, 2002: Simulation of the El Niño Southern Oscillation: results from the coupled model intercomparison project, *Clim. Dyn., 19,* 191–209.

AchutaRao, K., and K. R. Sperber, 2006: ENSO Simulation in Coupled Ocean-Atmosphere Models: Are the Current Models Better? *Climate Dyn.*, 10.1007/s00382-006-0119-7.

An, S.-I., and B. Wang. 2000: Interdecadal Change of the Structure of the ENSO Mode and Its Impact on the ENSO Frequency. *Journal of Climate*: Vol. 13, No. 12, pp. 2044–2055.Barnett, T. P., D. W. Pierce, M. Latif, and D. Dommenget, 1999: Interdecadal interactions between the tropics and midlatitudes in the Pacific basin. *Geophys. Res. Lett.,* **26,** 615–618.

Boyle, J. S. (2006), Upper level atmospheric stationary waves in the twentieth century climate of the Intergovernmental Panel on Climate Change simulations, *J. Geophys. Res.*, *111*, D14101, doi:10.1029/2005JD006612.

Davey, M. K., and coauthors, 2002: STOIC: a study of coupled model climatology and variability in tropical ocean regions, *Clim. Dyn., 18*, 403–420.

Delecluse, P., M. Davey, Y. Kitamura, S. Philander, M. Suarez, and L. Bengtsson, 1998: Coupled general circulation modeling of the tropical Pacific. *J. Geophys. Res.,* **103**, 14357–14373.

Gu, D., and S.G.H. Philander. 1995: Secular Changes of Annual and Interannual Variability in the Tropics during the Past Century. *Journal of Climate*: Vol. 8, No. 4, pp. 864–876.

Gu, D., and S. G. H. Philander, 1997: Interdecadal climate fluctuations that depend on exchanges between the tropics and extratropics. *Science,* **275,** 805–807.

Kleeman, R., J. P. McCreary Jr., and B. A. Klinger, 1999: A mechanism for generating ENSO decadal variability. *Geophys. Res. Lett.*, 26, 1743-1746.

Latif, M., and coauthors, 2001: ENSIP: the El Niño simulation intercomparison project, *Clim. Dyn., 18*, 255–276.

Lin, J. L., 2006: The double-ITCZ problem in IPCC AR4 coupled GCMs: Ocean-atmosphere feedback analysis. *J. Climate*, in press. Pdf file available at http://www.cdc.noaa.gov/people/jialin.lin/

Lin, J. L., G.N. Kiladis, B.E. Mapes, K.M. Weickmann, K.R. Sperber, W.Y. Lin, M. Wheeler, S.D. Schubert, A. Del Genio, L.J. Donner, S. Emori, J.-F. Gueremy, F. Hourdin, P.J. Rasch, E. Roeckner, and J.F. Scinocca, 2006a: Tropical intraseasonal variability in 14 IPCC AR4 climate models. Part I: Convective signals. *J. Climate*, **19**, 2665-2690.

Mak, M., 1995: Orthogonal Wavelet Analysis: Interannual Variability in the Sea Surface Temperature. *Bulletin of the American Meteorological Society*: Vol. 76, No. 11, pp. 2179–2186.

Rayner, N. A.; Parker, D. E.; Horton, E. B.; Folland, C. K.; Alexander, L. V.; Rowell, D. P.; Kent, E. C.; Kaplan, A., 2003: Global analyses of sea surface temperature, sea ice, and night marine air temperature since the late nineteenth century J. Geophys. Res., 108, No. D14, 4407 10.1029/2002JD002670.

Smith, T.M., and R.W. Reynolds, 2004: Improved Extended Reconstruction of SST (1854-1997). *J. Climate*, 17, 2466-2477.

Torrence, C., and G. P. Compo. 1998: A Practical Guide to Wavelet Analysis. *Bulletin of the American Meteorological Society*: Vol. 79, No. 1, pp. 61–78.Wang, B., 1995: Interdecadal changes in El Nino onset in the last four decades. *J. Climate,* **8,** 267–285.

Wang, B., and Y. Wang, 1996: Temporal structure of the Southern Oscillation as revealed by waveform and wavelet analysis. *J. Climate,* **9,** 1586–1598.

FIGURE CAPTIONS

Figure 1. Normalized Fourier spectrum of Nino3 SST for two observational datasets and 21 IPCC AR4 coupled GCMs.

Figure 2. Wavelet spectrum of Nino3 SST for two observational datasets and 21 IPCC AR4 coupled GCMs. Only power above the 95% confidence level is plotted.

Figure 3. Linear correlation with respect to Nino3 SST anomaly for SST anomaly (solid) and zonal wind stress (ZWS) anomaly (dashed) along the equator averaged between 5N-5S for the eight models in category 3. The black lines are for low-frequency regime, while the color lines are for high-frequency regime.

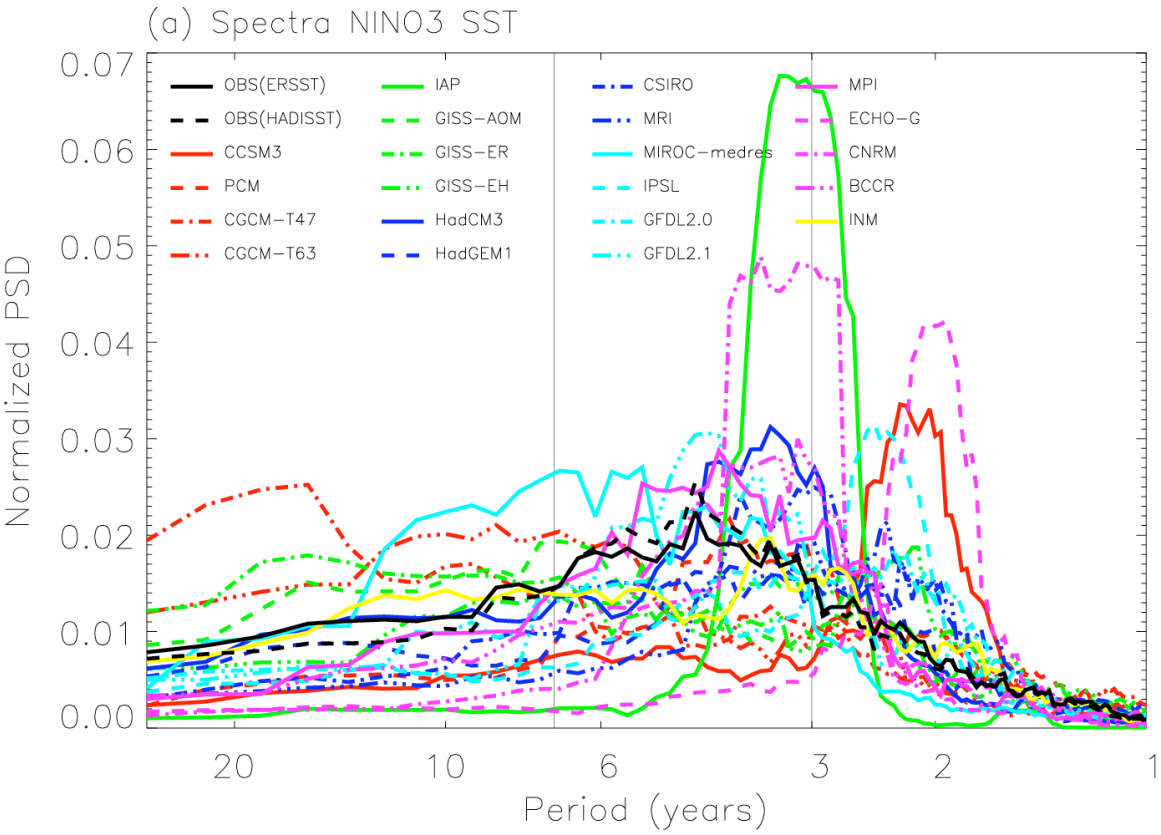

Figure 1. Normalized Fourier spectrum of Nino3 SST for two observational datasets and 21 IPCC AR4 coupled GCMs.

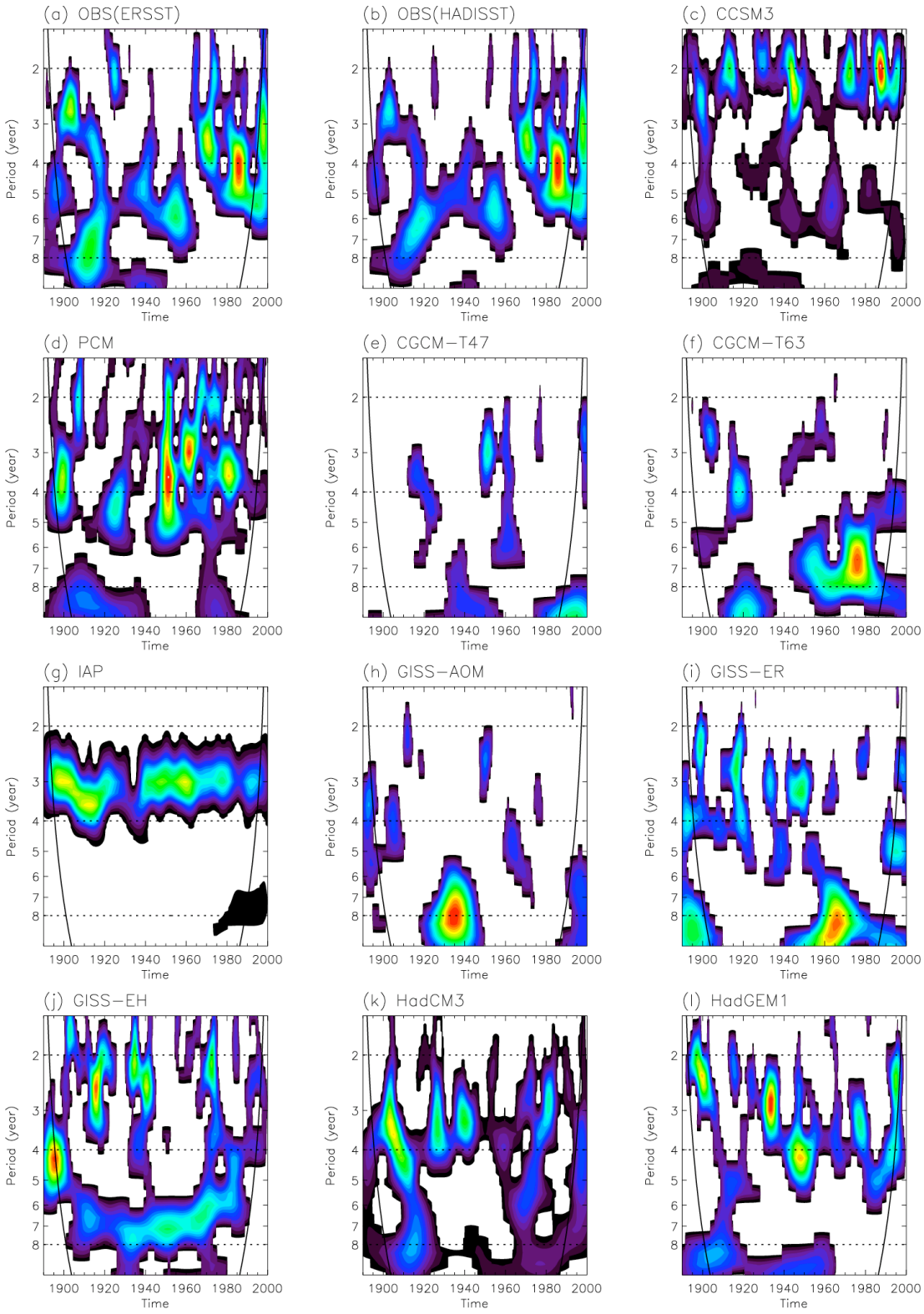

Figure 2. Wavelet spectrum of Nino3 SST for two observational datasets and 21 IPCC AR4 coupled GCMs. Only power above the 95% confidence level is plotted.

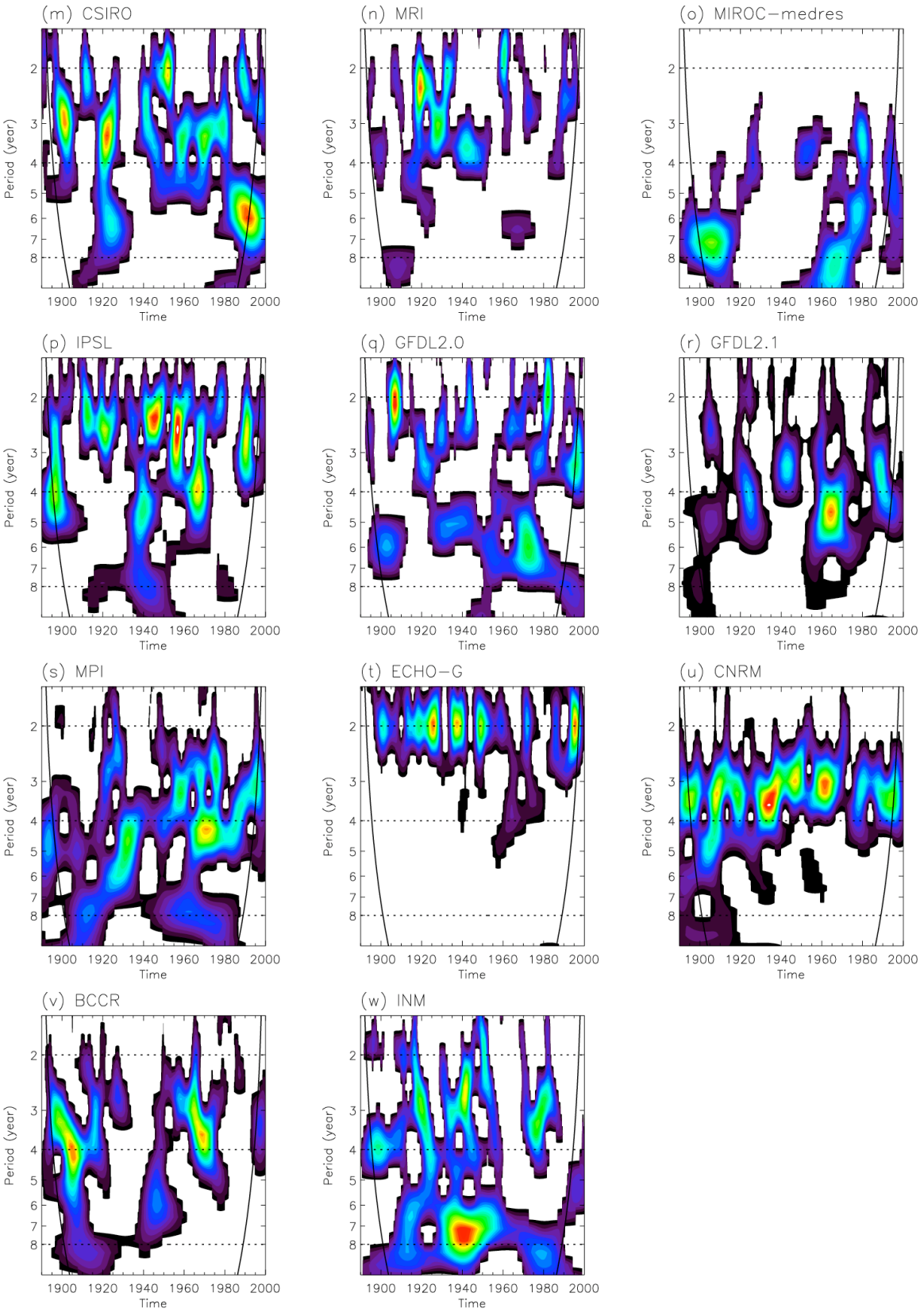

Figure 2. Continued.

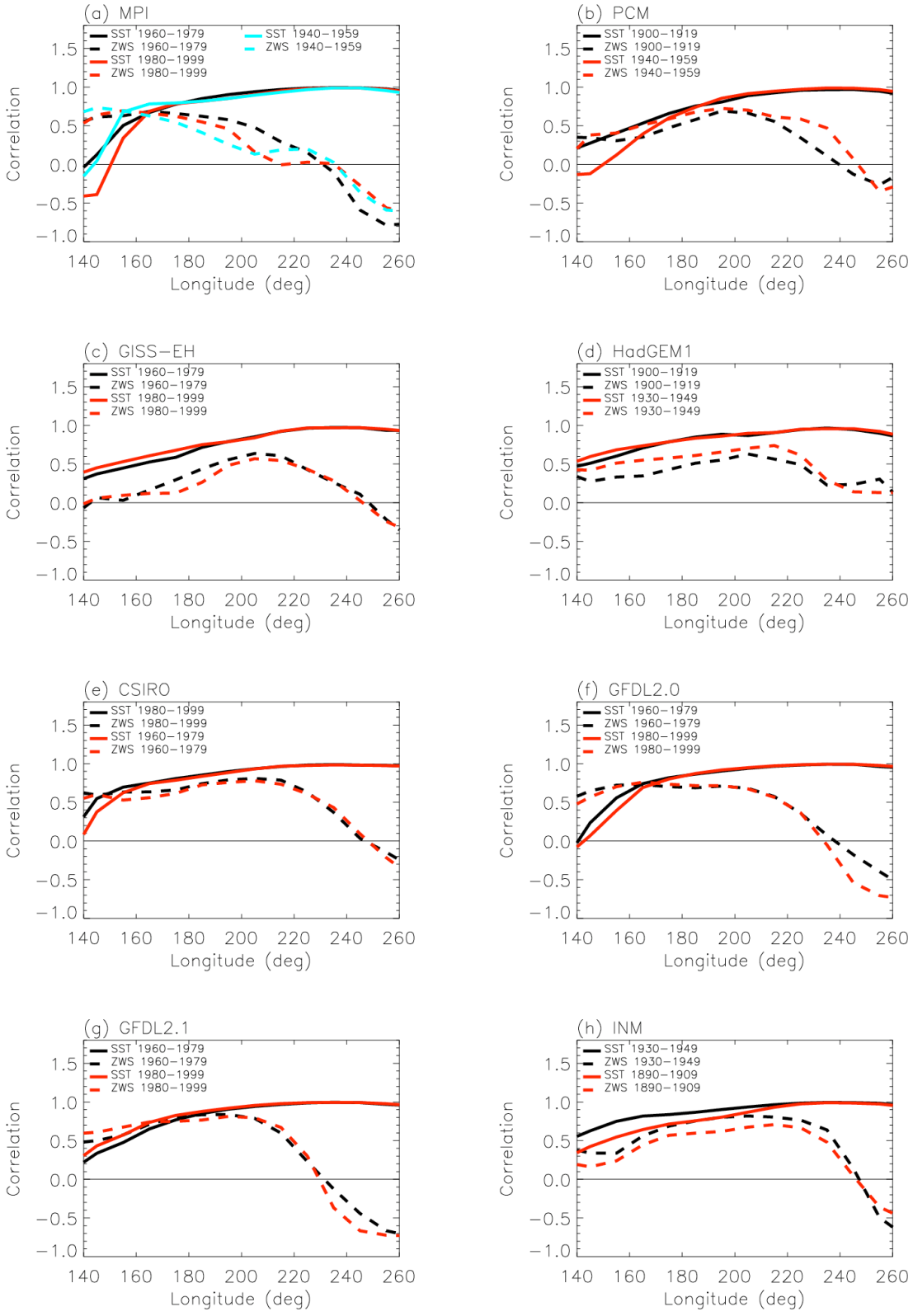

Figure 3. Linear correlation with respect to Nino3 SST anomaly for SST anomaly (solid) and zonal wind stress (ZWS) anomaly (dashed) along the equator averaged between 5N-5S for the eight models in category 3. The black lines are for low-frequency regime, while the color lines are for high-frequency regime.